Alpha-Actinin–containing Aggregates in Transformed Cells Are Highly Dynamic Structures

Shawn K. Stickel* and Yu-li Wang*‡

*Department of Molecular and Cellular Biology, National Jewish Center for Immunology and Respiratory Medicine, Denver, Colorado 80206; ‡Department of Biochemistry, Biophysics, and Genetics, University of Colorado Health Sciences Center, Denver, Colorado 80262

Abstract. Normal rat kidney cells infected with a Rous sarcoma virus (strain LA23) were used to study the dynamics of alpha-actinin–containing aggregates in transformed cells. Experiments were performed by microinjecting living cells with iodoacetamidotetramethylrhodamine alpha-actinin and allowing the fluorescent analogue to incorporate into cellular structures. Subsequent time-lapse recording indicated that the alpha-actinin–containing aggregates can undergo rapid formation, movement, and breakdown. In addition, experiments using the photobleaching recovery technique indicated that alpha-actinin molecules associated with the aggregates have a very high rate of exchange, whereas those associated with adhesion plaques in normal cells exchange much more slowly. The dynamic properties of alpha-actinin–containing aggregates may be closely related to the changes in cellular behavior upon oncogenic transformation.

MORPHOLOGICAL studies with cultured, oncogenically transformed cells have indicated an extensive reorganization of microfilament structures, including disappearance of stress fibers (Wang and Goldberg, 1976) and disruption of adhesion plaques (for a review see Maness, 1981). Many proteins associated with these structures, such as actin, alpha-actinin, vinculin (David-Pfeuty and Singer, 1980), talin (Burridge and Connell, 1983), and fimbrin (Carley et al., 1985) become localized into aggregates (also termed rosettes; Carley et al., 1981), which appear to lie close to weak attachments on the ventral surface (David-Pfeuty and Singer, 1980). Although such aggregates have been observed in a wide variety of transformed cells (Carley et al., 1981), their possible roles in transformation remain unclear. It is commonly believed that many important characteristics of transformed cells, such as increased motility, decreased spreading in culture, and lack of contact inhibition, can be directly related to the disruption of microfilament-containing structures.

To gain a better understanding of the nature of the possible roles of the actin- and alpha-actinin–containing aggregates in transformed cells, we have studied the dynamics of these aggregates in normal rat kidney (NRK)[1] cells transformed by Rous sarcoma virus (strain LA23). We have microinjected fluorescently labeled alpha-actinin into living cells. After incorporation of the analogue into cellular structures, the distribution of the aggregates was followed with a TV image intensifier. Furthermore, the rate of alpha-actinin exchange was studied by photobleaching the aggregates with a laser microbeam and recording the fluorescence recovery. Our experiments indicate that these aggregates are highly dynamic structures capable of changing their size and location very rapidly. The rate of protein exchange in these structures is also unusually high. These properties may be closely related to the changes in cellular behavior upon oncogenic transformation.

Materials and Methods

Cell Culture and Protein Preparation

NRK epithelial cells (NRK-52E; American Type Culture Collection, Rockville, MD) and Rous sarcoma virus–infected NRK cells (LA23; gift of R. L. Erikson, Harvard University) were grown in F12-K medium (KC Biological Inc., Lenexa, KS) supplemented with 10% FCS (KC Biological Inc.), 50 U/ml penicillin, and 50 μg/ml streptomycin. The cells were maintained in a 5% CO_2 environment at 34°C. Clones of LA23 cells were screened after temperature shift according to their morphological changes using phase-contrast microscopy and subsequently according to disruption of stress fibers and formation of aggregates using rhodamine–phalloidin (Molecular Probes Inc., Eugene, OR) staining. Cells were plated onto injection dishes (Wang, 1984) one day before experiments were performed.

Muscle alpha-actinin from frozen turkey gizzards and nonmuscle alpha-actinin from frozen calf thymus (Pel-Freez Biologicals, Rogers, AR) were purified and subsequently labeled with iodoacetamidotetramethylrhodamine (IATR; Molecular Probes Inc.) as described previously (Meigs and Wang, 1986). The ability of alpha-actinin to cross-link actin filaments was unaffected by fluorescent labeling, as determined by falling ball viscometry (McKenna et al., 1985).

Microinjection

Microinjection was performed as described by Graessmann et al. (1980) and cells were maintained on the microscope during the experiment as described previously (Wang, 1984). Experiments with LA23-NRK cells were per-

---

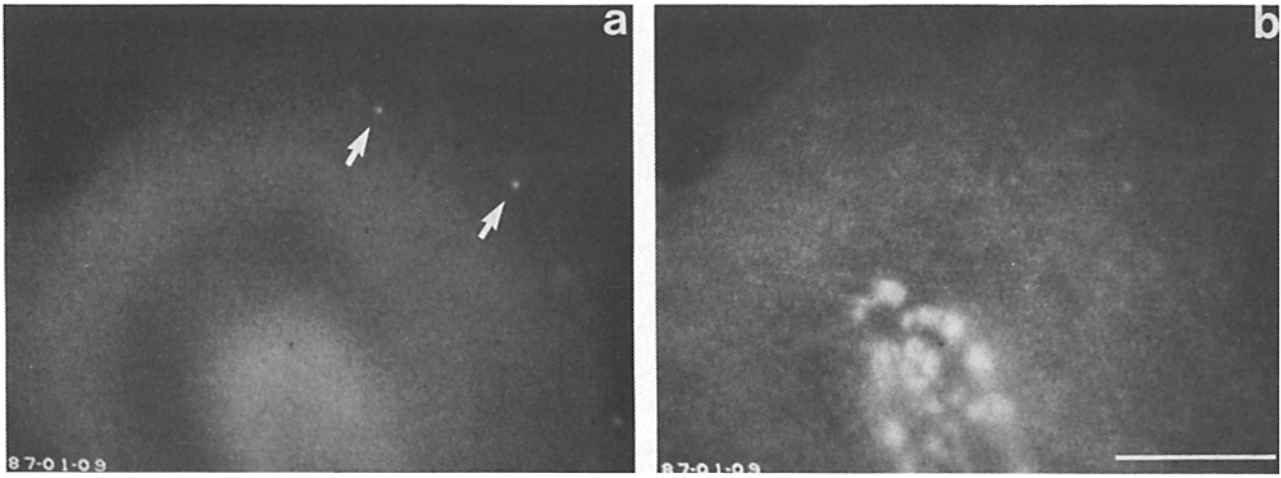1. *Abbreviations used in this paper:* IATR, iodoacetamidotetramethylrhodamine; NRK, normal rat kidney.

Figure 1. Location of aggregates by focusing through the cell. Fluorescent beads are used to mark the dorsal cell surface (*a; arrows*). A sharp image of the aggregates appears only after focusing downward through the cell to the ventral surface (*b*). Bar, 10 μm.

formed as soon as 10 min after microinjection because of the immediate incorporation of the analogue. No difference in results was detected with prolonged incubation after microinjection. For NRK-52E cells, the culture dish was returned to a regular CO_2 incubator for 2 h to allow incorporation of injected molecules.

Fluorescent Microscopy and Photobleaching

Fluorescent microscopy techniques were described previously (Wang, 1984). A 100× Neofluar objective (NA 1.30) was used for all experiments. For time-lapse sequences, images were recorded every 1–3 min by averaging
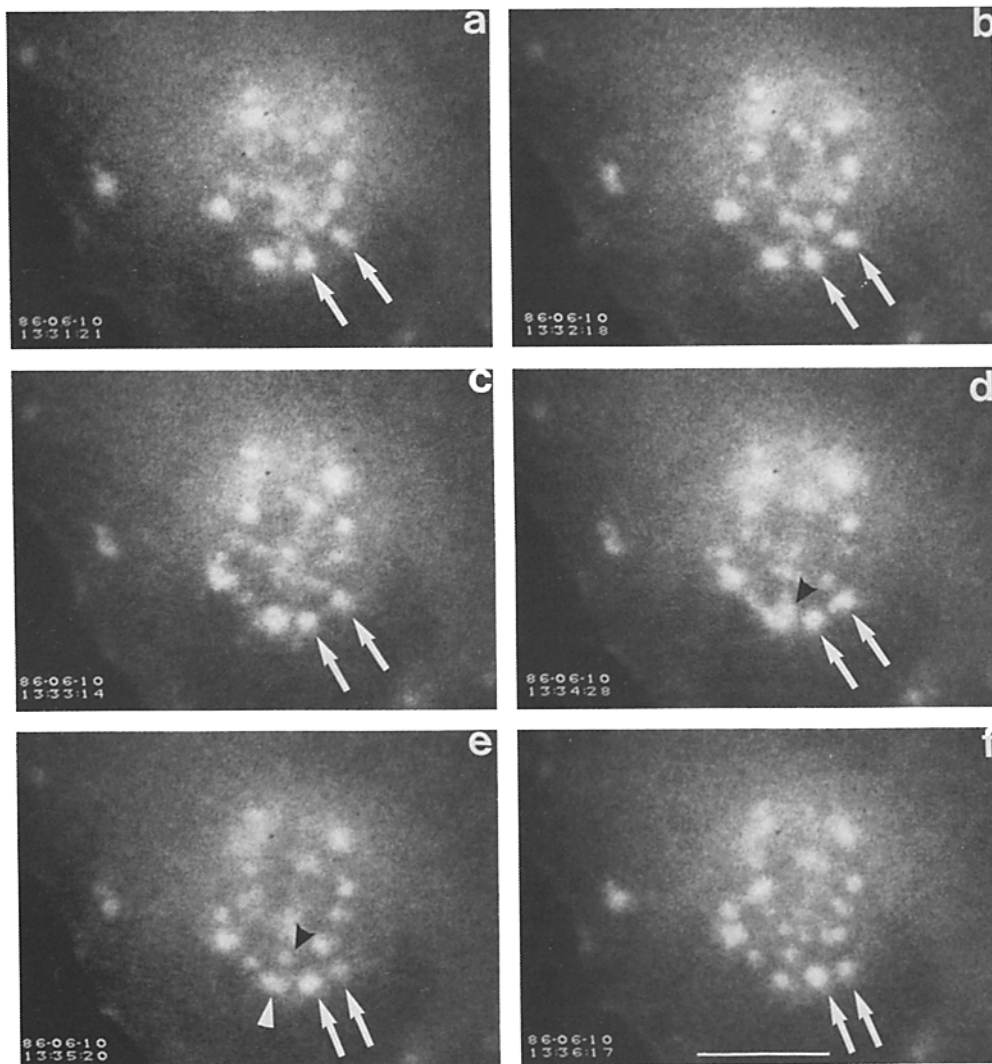

Figure 2. A 5-min time-lapse sequence which shows aggregates in an IATR alpha-actinin–injected LA23-NRK cell. Times of image recording are shown in the lower left-hand corner of each micrograph. The distance between two aggregates (*arrows*) has decreased from 3.5 to 2.4 μm. Their positions relative to neighboring aggregates have also changed over the period of observation. Another aggregate pinches to form two separate aggregates (*arrowheads*). Bar, 10 μm.
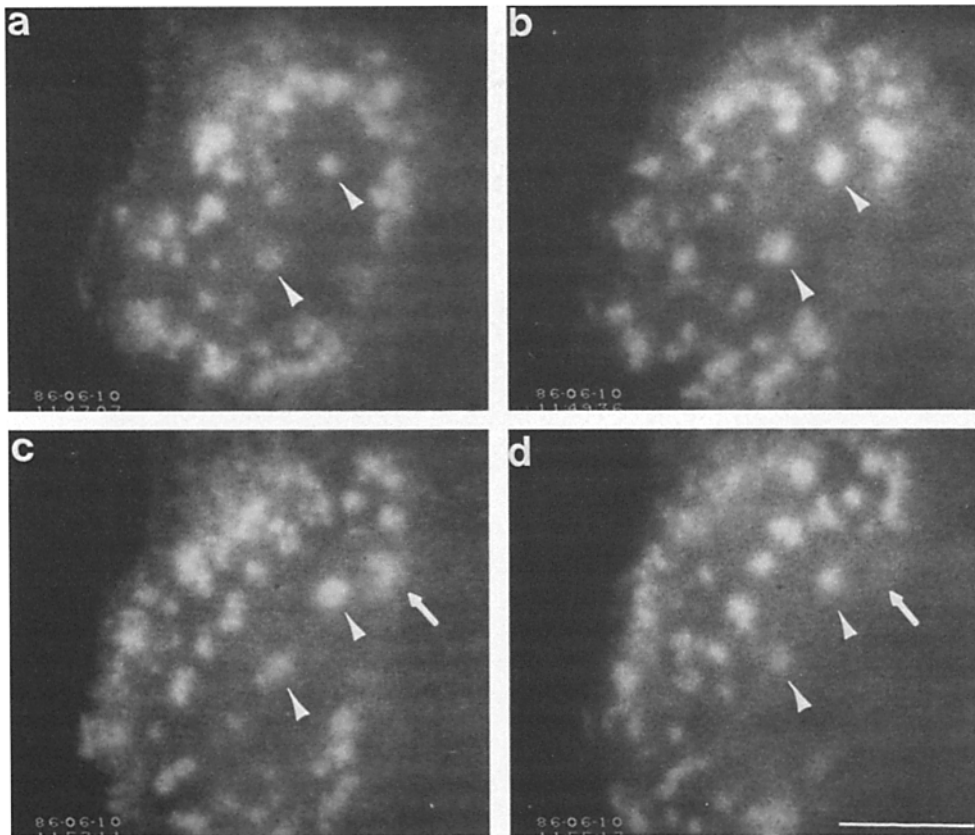
1522

Figure 3. An 8-min time-lapse sequence which shows aggregates in an IATR alpha-actinin–injected LA23-NRK cell. Times of image recording are shown in the lower left-hand corner of each micrograph. Dramatic changes occur in this group over an 8-min period. Two aggregates (*arrowheads*) show both intensity changes and relative movement during the course of recording. Arrows indicate an aggregate that disappears totally. Bar, 10 μm.

128 consecutive video frames as described previously (Wang, 1984). The rate of movement of the aggregates was estimated by marking their positions at different time points with a graphics tablet (GTCO, Rockville, MD), and calculating the distance of translocation.

Red fluorescent covasphere particles (MX-0.3 μm; Duke Scientific Corp., Palo Alto, CA) were prepared by washing and resuspending the beads in PBS solution at a concentration of 7.5 × 10^{10}/ml. A small volume of beads was then added to the culture dish and allowed to settle on the dorsal surface of the cells. Before recording images, the pneumatic table for the microscope was rocked gently to insure that the beads were resting on the cell surface. Unsettled beads moved readily away from the cell during this procedure.

Photobleaching was performed as previously described (McKenna et al., 1985) using a power of 75 mW and a laser pulse of 30–50 ms. The bleached area had a diameter of 4 μm. Fluorescence intensities were obtained by averaging eight consecutive video frames, integrating the total intensity within the bleached area, and subtracting out the background intensity. This process was performed before and repeatedly after photobleaching to obtain recovery kinetics. Images of the cell were monitored during this period of measurement to ensure that bleached aggregates remained unchanged in location and recovered to the prebleach size. The linearity of measurements was ~95%. Micrographs of fluorescence recovery were obtained by repeatedly averaging 32 consecutive frames and photographing the TV monitor screen using an Olympus OM-2 camera and a motor winder. The action of shutters, integration of intensities, and recording of images were all controlled by the image processing computer. Diffusion coefficients were calculated based on recovery halftimes according to Jacobsen et al. (1976).

Results

NRK cells, infected with a temperature-sensitive mutant of Rous sarcoma virus (strain LA23) and cultured at a permissive temperature, were used to study the dynamics of alpha-actinin–containing aggregates. Although alpha-actinin–containing aggregates are present in many types of transformed cells, the cell line used shows an excellent spreading capability which greatly facilitates microinjection and fluores-

cence microscopy. At the permissive temperature, adhesion plaques and stress fibers are either absent or greatly diminished, whereas aggregates are present in at least 80% of the cells and are often clustered into groups both in the central region and near the edge of the cell (Figs. 1 and 2; see also Carley and Webb, 1983). After microinjection, IATR alpha-actinin becomes incorporated into aggregates almost immediately. Although most experiments were performed with gizzard alpha-actinin, identical results were also obtained with nonmuscle (thymus) alpha-actinin.

By careful focusing, all fluorescent aggregates appeared to be located on the ventral (bottom) surface of the cell. This was further verified by marking the dorsal surface with red fluorescent beads, which had an appearance easily distinguishable from the aggregate. When focusing on the beads (Fig. 1 *a*), it was obvious the aggregates were present on a different focal plane. Sharp images of the aggregates appeared only after the microscope was refocused on the ventral surface (Fig. 1 *b*).

Using time-lapse recording, we found these aggregates to be highly dynamic. They are capable of movement (arrows, Fig. 2; arrowheads, Fig. 3), as well as changes in shape and size (arrowheads, Fig. 3). The rate of movement varied between 0 and 0.8 μm/min. In addition, one aggregate may pinch to form two or three (arrowheads, Fig. 2) or may appear or disappear (arrows, Fig. 3). These activities often resulted, within 5 min, in dramatic changes in the morphology of the entire group of aggregates (Fig. 3).

To determine whether the dynamic changes in morphology are coupled to a high rate of exchange of protein components, microinjected cells were photobleached to study the apparent mobility of alpha-actinin associated with the ag-
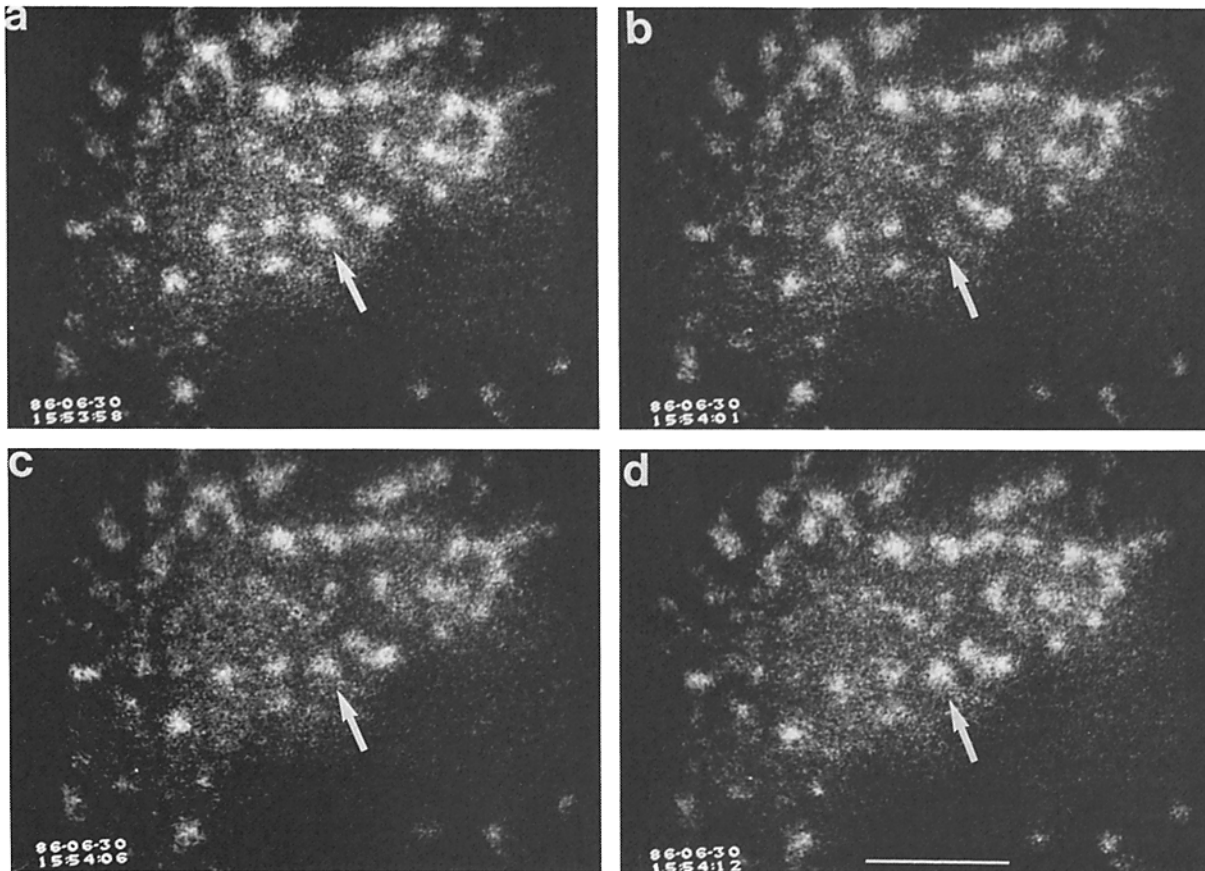
Figure 4. Photobleaching recovery of an aggregate in a IATR alpha-actinin–injected LA23-NRK cell. Times of image recording are indicated in the lower left-hand corner of each micrograph. An aggregate (*arrow*) is shown before (*a*), immediately after (*b*), 5 s after (*c*), and 11 s after (*d*) photobleaching. Extensive recovery is reached by the end of the period of recording. Bar, 10 μm.

gregates. Fig. 4 shows time-lapse images of an aggregate before and after photobleaching. Significant recovery is seen as soon as 5 s after photobleaching (Fig. 4 *c*) and extensive recovery within 11 s (Fig. 4 *d*). Because of the extremely high rate of recovery, we were able to measure the time course of many aggregates despite their continuous, slower movements. Based on recovery curves of additional photobleached cells, such as shown in Fig. 5, we found that the kinetics approximate a single exponential time course with an average halftime of 3.64 s (SD = 0.64, n = 11 in 7 cells). This corresponds to an apparent diffusion coefficient of 3 × 10^{-9} cm²/s. Similar kinetics were obtained when the surrounding cytoplasm was bleached either alone or together with an aggregate.

The mobility of alpha-actinin in adhesion plaques of untransformed NRK cells was also studied by photobleaching (Fig. 6). Adhesion plaques were chosen for comparison because of their apparent similarity to aggregates in transformed cells (see Discussion). They show very little recovery after 11 s, in comparison to the extensive recovery of aggregates over the same time period (Fig. 4 *d*). As late as 52 s after photobleaching (Fig. 6 *d*), fluorescence recovery is still far from complete. This slow recovery is also evident in the recovery curve of adhesion plaques. As shown in Fig. 7, the recovery consists of a small rapid phase over the first 10 s, which may represent the partial inclusion of ground cytoplasm, followed by an extensive slow phase. The total ex-

tent of recovery remained <50% at the end of the first min and increased slowly over the next 5 min.

Discussion

Based on available information on protein composition and location, there appears to be a strong resemblance between aggregates in transformed cells and adhesion plaques in normal cells. First, aggregates, which are seen on the ventral cell surface (Fig. 1), have been shown to correspond to gray plaques in interference reflection microscopy images (David-Pfeuty and Singer, 1980; also our unpublished observation). This indicates that they are probably involved in the association of the cell with the substrate, although, based on the darkness of these plaques, the contact appears to be weaker than that mediated by adhesion plaques (Carley and Webb, 1983). Second, many proteins found in adhesion plaques, including actin, alpha-actinin, vinculin, talin, and fimbrin are also concentrated in the aggregates in transformed cells (David-Pfeuty and Singer, 1980; Burridge and Connell, 1983; and Carley et al., 1985). Notably, vinculin and talin are concentrated specifically at adhesion plaques and cell–cell contact sites in normal cells (Geiger, 1979; Burridge and Feramisco, 1980; and Burridge and Connell, 1983).

However, compared to adhesion plaques, aggregates have a much higher rate of morphological reorganization and protein exchange. Adhesion plaques in normal cells are known
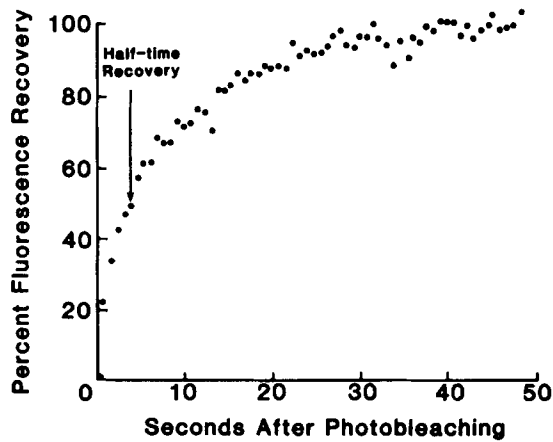
Figure 5. Time course of fluorescence recovery after photobleaching an aggregate. Time 0 represents the first time point measured after photobleaching. Halftime of fluorescence recovery for this aggregate is estimated to be 4.0 s.

Figure 7. Time course of fluorescence recovery after photobleaching of an adhesion plaque in NRK-52E cell. Time 0 represents the first time period measured after photobleaching. At the end of 50 s, fluorescence recovery has reached only 45%.

to be relatively stationary structures. They appear to assemble near the leading edge of the cell, show little movement during cell locomotion while most other structures move forward, and disassemble when they lag far behind the leading edge (Izzard and Lochner, 1980). In contrast, aggregates can appear and disappear, even far away from the edge of the cell, within a 5-min period. Furthermore, they also undergo rapid movement and splitting during their life span.

These differences between adhesion plaques and aggregates may be related to the stability of their proteins. Indeed, using fluorescence recovery after photobleaching, we found that essentially 100% of alpha-actinin molecules in the aggregates are highly mobile, with a recovery kinetic curve in-
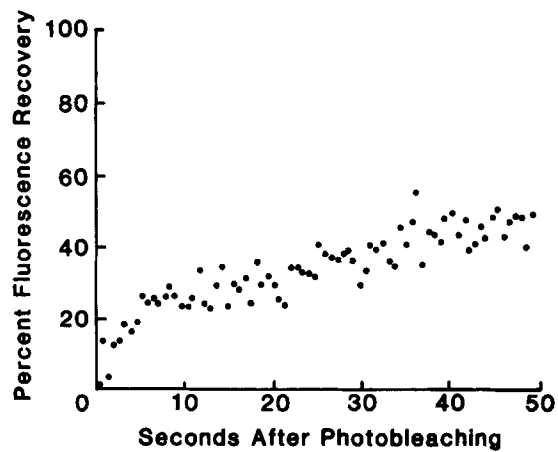
distinguishable from that of the surrounding cytoplasm. Therefore, alpha-actinin and possibly other protein components can exchange at a very high rate in and out of the aggregates, and the rate-limiting step for the exchange may be the diffusion of molecules in the cytoplasm. On the contrary, similar experiments on adhesion plaques show very limited recovery over a prolonged period of time, consistent with the previous report that at least 60% of alpha-actinin molecules have a very low mobility (Geiger et al., 1984).

Several factors may contribute to the difference in stability between aggregates and adhesion plaques. It has been shown that the aggregates contain a high concentration of protein tyrosine kinase (e.g., David-Pfeuty and Singer, 1980; Chen
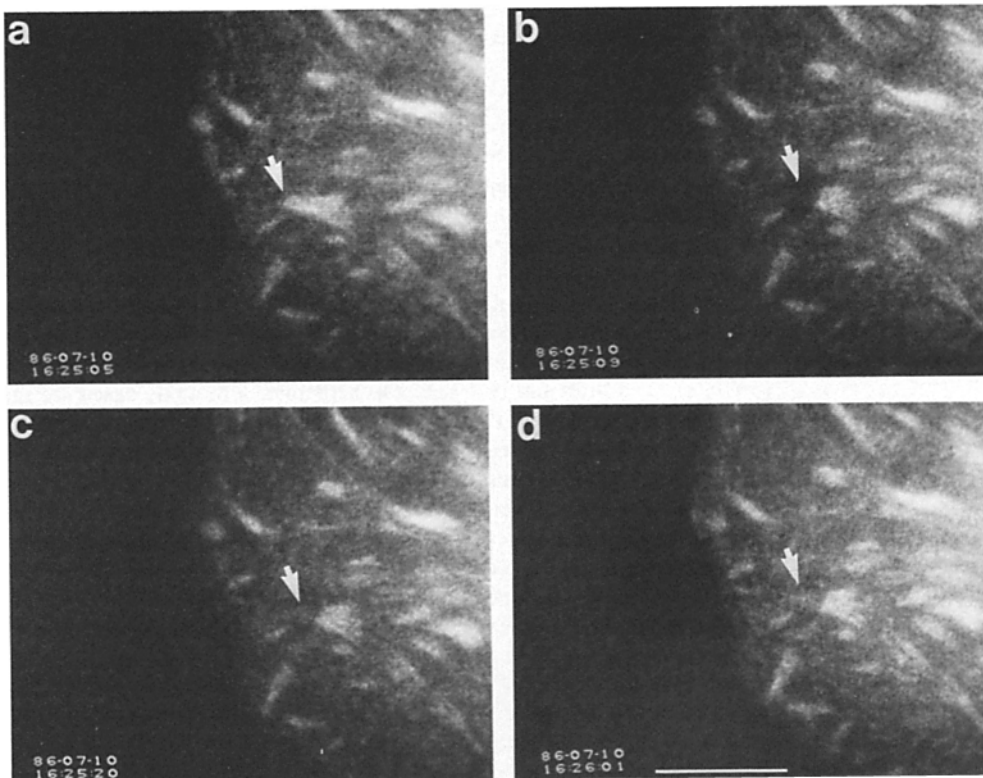

Figure 6. Photobleaching recovery of an adhesion plaque in a nontransformed NRK-52E cell injected with IATR alpha-actinin. Times of image recording are indicated in the lower left-hand corner of each micrograph. The adhesion plaque (*arrow*) is shown before (*a*), immediately after (*b*), 11 s after (*c*), and 52 s after (*d*) photobleaching. Even at the end of the sequence, recovery is still far from being complete. Bar, 10 μm.

et al. 1986). An increase in the level of protein phosphorylation may, therefore, affect the stability of the structure. Alternatively, destabilization of structures may be due to extracellular proteases, which are highly active in transformed cells under the aggregates and cause the degradation of the extracellular matrix (Chen et al., 1984). This may result in a decrease in the adhesion of cells and an increase in the mobility of proteins in the adjacent cytoplasm. Future experiments, such as studying the effect of exogenously added fibronectin on the mobility of proteins in aggregates, may shed some light on the actual mechanism involved.

If the aggregates are indeed related to adhesion plaques, the question arises as to the exact relationship between them. David-Pfeuty and Singer (1980) have suggested that aggregates do not simply represent residues of disrupted stress fibers and adhesion plaques in the transformed cell, but rather, weakened (and possibly destabilized) adhesion plaques. Alternatively, Bershadsky et al. (1985) reported that Rous sarcoma virus transformation affects the formation of mature adhesion plaques, but not the formation of nascent contact sites with the substrate. Therefore, it is also possible that aggregates represent nascent adhesion structures that are unstable and incapable of developing into adhesion plaques.

The disruption of strong adhesion sites and the formation of weak, unstable substrate contacts can clearly account for the less spread and less stable morphology of transformed cells. In addition, since adhesion plaques are normally formed near the active lamellipodia, the rapid assembly and disassembly of aggregates at random sites of transformed cells implies that transformed cells have either lost or greatly altered the control mechanism for the locomoting machinery.

References

Bershadsky, A. D., I. S. Tint, A. A. Neyfakh, and J. M. Vasiliev. 1985. Focal contacts of normal and RSV-transformed quail cells. *Exp. Cell Res.* 158: 433-444.

Burridge, K., and L. Connell. 1983. Talin: a cytoskeletal component concentrated in adhesion plaques and other sites of actin-membrane interaction. *Cell Motil.* 3:405-417.

Burridge, K., and J. R. Feramisco. 1980. Microinjection and localization of a 130K protein in living fibroblasts: a relationship to actin and fibronectin. *Cell.* 19:587-595.

Carley, W. W., L. S. Barak, and W. W. Webb. 1981. F-actin aggregates in transformed cells. *J. Cell Biol.* 90:797-802.

Carley, W. W., A. Bretscher, and W. W. Webb. 1985. F-actin aggregates in transformed cells contain α-actinin and fimbrin but apparently lack tropomyosin. *Eur. J. Cell Biol.* 39:313-320.

Carley, W. W., and W. W. Webb. 1983. F-actin aggregates may activate transformed cell surfaces. *Cell Motil.* 3:383-390.

Chen, W.-T., K. Olden, B. A. Bernard, and F. F. Chu. 1984. Expression of transformation-associated protease(s) that degrade fibronectin at cell contact sites. *J. Cell Biol.* 98:1546-1555.

Chen, W.-T., J. Wang, T. Hasegawa, S. S. Yamada, and K. M. Yamada. 1986. Regulation of fibronectin receptor distribution by transformation, exogenous fibronectin, and synthetic peptides. *J. Cell Biol.* 103:1649-1661.

David-Pfeuty, T., and S. J. Singer. 1980. Altered distributions of the cytoskeletal proteins vinculin and α-actinin in cultured fibroblasts transformed by Rous sarcoma virus. *Proc. Natl. Acad. Sci. USA.* 77:6687-6691.

Geiger, B. 1979. A 130K protein from chicken gizzard: its localization at the termini of microfilament bundles in cultured chicken cells. *Cell.* 18:193-205.

Geiger, B., Z. Avnur, G. Rinnerthaler, H. Hinssen, and V. J. Small. 1984. Microfilament-organizing centers in areas of cell contact: cytoskeletal interactions during cell attachment and locomotion. *J. Cell Biol.* 99:83s-91s.

Graessman, A., M. Graessman, and C. Mueller. 1980. Microinjection of early SV40 DNA fragments and T antigen. *Methods Enzymol.* 65:816-825.

Izzard, C. S., and L. R. Lochner. 1980. Formation of cell-to-substrate contacts during fibroblast motility: an interference-reflexion study. *J. Cell Sci.* 42: 81-116.

Jacobsen, K., Z. Derzko, E.-S. Wu, Y. Hou, and G. Poste. 1976. Measurement of the lateral mobility of cell surface components in single, living cells by fluorescence recovery after photobleaching. *J. Supramol. Struct.* 5:565-576.

Maness, P. F. 1981. Actin structure in fibroblasts – its possible role in transformation and tumorgenesis. *In* Cell and Muscle Motility, Vol. I. R. M. Dowben and J. W. Shaw, editors. Plenum Publishing Corp., New York. 335-373.

McKenna, N. M., J. B. Meigs, and Y.-L. Wang. 1985. Exchangeability of alpha-actinin in living cardiac fibroblasts and muscle cells. *J. Cell Biol.* 101:2223-2232.

Meigs, J. B., and Y.-L. Wang. 1986. Reorganization of alpha-actinin and vinculin induced by a phorbol ester in living cells. *J. Cell Biol.* 102:1430-1438.

Wang, E., and A. R. Goldberg. 1976. Changes in microfilament organization and surface topography upon transformation of chick embryo fibroblasts with Rous sarcoma virus. *Proc. Natl. Acad. Sci. USA.* 73:4065-4069.

Wang, Y.-L. 1984. Reorganization of actin filament bundles in living fibroblasts. *J. Cell Biol.* 99:1478-1485.